Available online at www.sciencedirect.com
ScienceDirect
European Journal of Protistology 43 (2007) 265–279
European Journal of PROTISTOLOGY
www.elsevier.de/ejop

# Classification of the peritrich ciliate *Opisthonecta matiensis* (Martín-Cereceda et al. 1999) as *Telotrochidium matiense* nov. comb., based on new observations and SSU rDNA phylogeny

Mercedes Martín-Cereceda[a,*,1], Almudena Guinea[b], Elisa Bonaccorso[c], Patricia Dyal[a], Gianfranco Novarino[a], Wilhelm Foissner[d]

[a]*Department of Zoology, The Natural History Museum, Cromwell Road, London SW7 5BD, UK*
[b]*Departamento de Microbiologia III, F. Biologia, UCM, Madrid 28040, Spain*
[c]*Natural History Museum and Biodiversity Research Center, University of Kansas, Lawrence, KS 66045, USA*
[d]*Universität Salzburg, FB Organismische Biologie, A-5020 Salzburg, Austria*

Received 15 February 2007; received in revised form 19 April 2007; accepted 23 April 2007

## Abstract

New observations on *Opisthonecta matiensis* Martín-Cereceda et al. [1999. Description of *Opisthonecta matiensis* n. sp. (Protozoa, Ciliophora), a new peritrich ciliate from wastewater. J. Eukaryot. Microbiol. 46, 283–289] especially the lack of an epistomial membrane, reveal that the species does not belong to the genus *Opisthonecta*, but to *Telotrochidium,* the other genus within the family Opisthonectidae Foissner, 1975. The contractile vacuole and the cytopyge are on the dorsal wall of the vestibulum and the trochal band is limited distally and proximally by rows of narrowly spaced pellicular pores. Thus the species is redefined as *Telotrochidium matiense* nov. comb. The morphological, cortical and nuclear events occurring during conjugation are illustrated, compared with those in other species, and phylogenetically discussed. Invariably, the microconjugants attach to and penetrate the lateral side of the macroconjugants. Nuclear processes are very similar to those reported from other peritrichs. The small subunit rRNA gene (SSU rDNA) is sequenced and the phylogeny within Opisthonectidae and peritrichs examined. *T. matiense* is more closely related to *Epistylis* (63% Maximum Parsimony (MP), 85% Maximum Likelihood (ML)) than to any other genus, while another representative of the family, viz., *Opisthonecta henneguyi,* is closely related to *Vorticella microstoma*, *Astylozoon enriquesi* and clone RT3n18 (100% MP, 100% ML). Morphology and gene sequences suggest that *Telotrochidium* and *Opisthonecta* have derived from different lineages of stalked peritrichs: *Opisthonecta* could have arisen from peritrichs with stalk myonemes, while *Telotrochidium* probably evolved from peritrichs without stalk myonemes.
© 2007 Elsevier GmbH. All rights reserved.

***Keywords:*** Ciliophora; Conjugation; Peritrichia; Phylogeny of peritrichs; Redescription; *Telotrochidium*

*Corresponding author. Fax: +1 785 8645321.
*E-mail address:* cereceda@ku.edu (M. Martín-Cereceda).
[1]Current address: Department of Ecology and Evolutionary Biology, Haworth Hall, 1200 Sunnyside Avenue, University of Kansas, Lawrence, KS 66045, USA.

0932-4739/$ - see front matter © 2007 Elsevier GmbH. All rights reserved.
doi:10.1016/j.ejop.2007.04.003

## Introduction

Classification of peritrich ciliates has been based largely on morphological features revealed by *in vivo* observation, silver impregnation, and electron microscopy. Modern molecular and phylogenetic methods – especially direct comparison of phylogenetically informative genes – are now used widely for the reconstruction of phylogenies not only within the peritrichs but also across the entire spectrum of protists (e.g. Cavalier-Smith 2004; Cavalier-Smith and Chao 2006; Moon-van der Staay et al. 2006; Schlegel 2003). Specifically within the peritrichs, it has been suggested that the small subunit rRNA gene (SSU rDNA) is an important marker for identifying species of *Vorticella* (Itabashi et al. 2002).

In the family Opisthonectidae, erected by Foissner (1975), to which the present study pertains, only one SSU rDNA sequence has been published (Greenwood et al. 1991), viz., that of *Opisthonecta henneguyi*, type species of the genus (Fauré-Frémiet 1906; Foissner 1975). Results suggested that peritrichs are clearly distinct from other Oligohymenophora. More recently, SSU rDNA sequences from several other peritrichs have been added (Clamp and Williams 2006; Gong et al. 2006; Itabashi et al. 2002; Miao et al. 2001, 2002, 2004). Although these data supported the idea that the subclass Peritrichia is monophyletic, a very recent study which incorporated sequences of the mobilid peritrichs (Trichodina), doubted their monophyly (Gong et al. 2006). Therefore, the phylogenetic relationships between peritrichs are still under discussion and in need of further investigation (Clamp and Williams 2006; Gong et al. 2006; Itabashi et al. 2002; Miao et al. 2004).

The subject of the present study is a peritrich ciliate described as *Opisthonecta matiensis* by Martín-Cereceda et al. (1999). It is a representative of the free-swimming sessilid genus *Opisthonecta* Fauré-Frémiet, 1906, which has been included along with the genus *Telotrochidium* Kent, 1881, in the family Opisthonectidae by Foissner (1975). Based on new morphological and molecular data (SSU rDNA), we transfer *O. matiensis* to the genus *Telotrochidium*, which appears closely related to stalked peritrichs of the family Epistylidae.

Detailed information on sexual processes in free-swimming sessilid peritrichs have only been reported twice and for the same species, viz., *O. henneguyi* (Rosenberg 1940; Sola et al. 1989). In this paper, we illustrate the morphological, cortical and nuclear changes occurring during the conjugation of *Telotrochidium matiense*, compare them with other species of peritrichs, and discuss their phylogenetic significance.

## Material and methods

### Material

Originally, *T. matiense* was isolated from the inlet water to a rotating biological contactor wastewater treatment plant (Martín-Cereceda et al. 1999). The species has been maintained for more than 10 years in laboratory culture using Cerophyl®/0.2 μm filtered Volvic® mineral water (3/7 v/v) supplied periodically with a suspension of *Vibrio natriegens* (Colección Española de Cultivos Tipo, CECT 526). The type culture has been deposited at the Culture Collection of Algae and Protozoa (CCAP, accession number 1655/2) and was used for the present investigations.

### Light and electron microscopy; conjugation

Living cells were studied as described by Foissner (1991), using a high-power oil immersion objective (100 ×) and differential interference contrast. Protargol impregnation was performed following protocol A described in Foissner (1991) using, however, a different fixative, viz., 70% ethyl alcohol. This simple fixation gives excellent results for several ciliates, especially all peritrichs tested so far. Drawings of live specimens were based on free-hand sketches and micrographs, while a drawing device was used for preparations.

Only a culture has been deposited as a type (see above and Martín-Cereceda et al. 1999). Thus, we deposited in the Oberösterreichischen Landesmuseum in Linz (LI), Austria, three type slides with protargol-impregnated specimens and two type slides with silver nitrate-impregnated cells (Foissner 1991) from the type culture. Some relevant specimens are marked by black ink circles on the coverslip.

Conjugation begins about 60–72 h after re-inoculation in fresh medium, and the entire process lasts about 48 h in total. To follow the various conjugation steps, 50–60 cells were harvested from conjugating cultures at elapsed times, impregnated with pyridinated silver carbonate (Fernández-Galiano 1994), and observed using an Olympus BH-2 microscope. Observations on living cells were carried out using an Olympus BX50 microscope with phase-contrast illumination. For scanning electron microscopy (SEM), cells were fixed with EM-grade glutaraldehyde (1.5% final concentration) overnight at 4 °C, and then placed for 2–3 h on coverslips previously coated with poly-L-lysine solution (Sigma-Aldrich, 15 min). Cells were post-fixed using osmium tetroxide (2% final concentration), dehydrated in a graded isopropanol series (30%, 50%, 70%, 90%, 95%, 98% and 100%), and chemically dried using hexamethyldisilazane (HMDS, Sigma-Aldrich) at 100%, twice for

10 min each. Observations were made using a Philips XL-30 field emission SEM.

## DNA extraction, amplification and sequencing

Cells were grown for four days in Cerophyl medium and pelleted at 5000*g* for 10 min. The DNA was extracted using a modified protocol from Fuhrman et al. (1988), that is, the pellet was lysed in 500 µl of TE/1% SDS buffer (10 mM Tris-HCl pH 7.5; 1 mM EDTA; 1% sodium dodecyl sulphate) and the lysate then extracted with an equal volume of phenol (pH 7.9), followed by two extractions with chloroform/iso-amyl alcohol (24:1). The genomic DNA (aqueous phase) was then concentrated to a volume of 20 µl using the Amicon Microcon® YM-100 centrifugal filter unit according to the manufacturer's protocol (Millipore). The eukaryotic universal primers forward 5′F AYC TGG TTG ATY YTG CCA GY and reverse 3′R TGA TCC ATC TGC AGG TTC ACC were used to amplify the full-length eukaryotic SSU rDNA gene (Embley et al. 1992). Fifty µl PCR amplifications were performed, using 25 µl of AmpliTaq Gold® PCR master mix (which contains 0.05 U/µl AmpliTaq Gold® DNA Polymerase, Gold buffer (30 mM TrisHCl pH 8.05, 100 mM KCl), 5 mM $MgCl_2$ and 400 µM of each dNTP), 20 pmol of each primer, 1 µl of template DNA solution, and sterile Sigma Millipure water to 50 µl total volume. Thermal cycling was performed with an initial denaturation for 1 min at 95 °C; then 10 cycles of 1 min at 94 °C, 30 s at 50 °C, 2 min at 72 °C; then 20 cycles of 30 s at 92 °C, 30 s at 50 °C, 2 min 30 s at 72 °C; and a final extension of 30 min at 72 °C.

PCR products were purified using the QIAquick PCR Purification Kit (Qiagen) and cloned into pGEM®-T Easy Vector (Promega). *Escherichia coli* JM109® high-efficiency competent cells were transformed for plasmid propagation according to the manufacturer's protocol. Plasmid DNA was isolated from six clones using the QIA prep® Spin Miniprep Kit (Qiagen). Clones containing the SSU rDNA gene insert were identified by digestion of the plasmid DNA with the restriction enzyme EcoR1. Protocols for cycle sequencing (BigDye® Terminator v1.1 Cycle Sequencing Kit, Applied Biosystems) followed manufacturer's instructions except that 1 µl of big dye was used in a total reaction volume of 10 µl. Clones were sequenced with the M13 forward and reverse vector-based primers and primers selected from Elwood et al. (1985). Thermal cycling was performed with an initial denaturation for 5 min at 96 °C, followed by 25 cycles of 10 s at 96 °C, 10 s at 50 °C, and 4 min at 60 °C. Sequence reactions were purified using the Montage PCR96 Cleanup Plate Kit (Millipore) and run on a 3730 DNA analyzer from Applied Biosystems. Sequences were verified by forward and reverse comparisons, and assembled and edited using Sequencher (vers. 4.5, Gene Codes, Ann Arbor, MI).

**Table 1.** Ciliate species included in the phylogenetic trees of this study

| Species | Accession number | Reference |
|---|---|---|
| *Anophryoides haemophila* | U51554 | Ragan et al. (1996) |
| *Astylozoon enriquesi* | AY049000 | Strüder-Kypke unpubl. |
| *Campanella umbellaria* | AF401524 | Miao et al. (2004) |
| *Carchesium polypinum* | AF401522 | Miao et al. (2004) |
| *Cohnilembus verminus* | Z22878 | Dyal et al. unpubl. |
| *Colpidium campylum* | X56532 | Greenwood et al. (1991) |
| *Cyclidium plouneouri* | U27816 | Embley et al. (1995) |
| *Epicarchesium abrae* | DQ190462 | Li and Song unpubl. |
| *Epistylis chrysemydis* | AF335514 | Miao et al. (2001) |
| *Epistylis galea* | AF401527 | Miao et al. (2004) |
| *Epistylis hentscheli* | AF335513 | Miao et al. (2001) |
| *Epistylis plicatilis* | AF335517 | Miao et al. (2001) |
| *Epistylis* sp. Miyagi | AB074080 | Itabashi et al. (2002) |
| *Epistylis urceolata* | AF335516 | Miao et al. (2001) |
| *Epistylis wenrichi* | AF335515 | Miao et al. (2001) |
| *Frontonia vernalis* | U97110 | Hirt et al. unpubl. |
| *Glaucoma chattoni* | X56533 | Greenwood et al. (1991) |
| *Ichthyophthirius multifiliis* | U17354 | Wright and Lynn (1995) |
| *Loxodes magnus* | L31519 | Hirt et al. (1995) |
| *Metanophrys similis* | AY314803 | Shang et al. (2006) |
| *Opercularia microdiscum* | AF401525 | Miao et al. (2004) |
| *Ophrydium versatile* | AF401526 | Miao et al. (2004) |
| *Opisthonecta henneguyi* | X56531 | Greenwood et al. (1991) |
| *Paramecium caudatum* | AF217655 | Strüder-Kypke et al. (2000) |
| *Paramecium bursaria* | AF100314 | Strüder-Kypke et al. (2000) |
| *Paramecium calkinsi* | AF100310 | Strüder-Kypke et al. (2000) |
| *Paramecium duboscqui* | AF100312 | Strüder-Kypke et al. (2000) |
| *Paramecium polycaryum* | AF100313 | Strüder-Kypke et al. (2000) |
| *Pseudocohnilembus marinus* | Z22880 | Dyal et al. unpubl. |
| *Pseudovorticella punctata* | DQ190466 | Li and Song, unpubl. |
| *Pseudovorticella sinensis* | DQ845295 | Li and Song unpubl. |
| RT3n18 | AY082994 | Amaral-Zettler et al. (2002) |
| *Stylonychia pustulata* | X03947 | Sogin et al. (1986) |
| *Tetrahymena australis* | X56167 | Sogin et al. (1986) |
| *Tetrahymena corlissi* | U17356 | Wright and Lynn (1995) |
| *Tetrahymena farleyi* | AF184665 | Lynn et al. (2000) |
| *Vaginicola crystallina* | AF401521 | Miao et al. (2004) |
| *Vorticella campanula* | AF335518 | Miao et al. (2001) |
| *Vorticella convallaria* | AF070700 | Williams unpubl. |
| *Vorticella convallaria* | AB074081 | Itabashi et al. (2002) |
| *Vorticella convallaria* | AB074082 | Itabashi et al. (2002) |
| *Vorticella fusca* | DQ190468 | Li and Song unpubl. |
| *Vorticella microstoma* | AF070701 | Williams unpubl. |
| *Vorticella* sp. Tianjin | AB074083 | Itabashi et al. (2002) |
| *Zoothamnium arbuscula* | AF401523 | Miao et al. (2004) |
| *Zoothamnopsis sinica* | DQ190469 | Li and Song unpubl. |

Subsequent comparisons of the nucleotide sequence were performed with the BLAST algorithm.

## Sequence availability and phylogenetic analyses

Species and GenBank accession numbers of the nucleotide sequences used are listed in Table 1. The

sequence alignments were performed using CLUSTAL-X (Thompson et al. 1997) and corrected in MacClade vers. 4.0 (Maddison and Maddison 2000). In total, the SSU rDNA sequences of 47 species were compared. In all analyses, features were considered as unordered and gaps treated as missing characters. Phylogenetic analyses were conducted using Maximum Parsimony (MP) and Maximum Likelihood (ML) in PAUP (Swofford 2000). The MP analysis was carried out using heuristic searches (100 stepwise random additions with TBR branch-swapping). Clade support was estimated via 100 bootstrap pseudo-replicates (Felsenstein 1985) with the aforementioned search options. Previous to ML analysis, the best-fit model of evolution and parameter values for the SSU rDNA was selected using ModelTest vers. 3.7 (Posada and Crandall 1998). A general time reversible model (Yang 1994a), with $\gamma$-distributed rates across sites and invariant sites (Yang 1994b), was estimated from the data and applied to the ML analysis. The ML tree was obtained using 100 stepwise random additions with TBR branch-swapping. Node support was assessed via 100 bootstrap pseudo-replicates with initial trees generated by neighbor joining. Tree visualization was performed with Tree View (Page 1996).

## Results

### Supplementary observations on the morphology of *Telotrochidium matiense* (Martín-Cereceda et al., 1999) nov. comb.

The accurate reinvestigation of specimens from the type culture showed that the original description is almost perfect. Thus, a redescription is not necessary. However, two important details were misinterpreted, making it necessary to amend the diagnosis and to provide improved images (Figs 1 and 2).

A first mistake in the original description concerns the epistomial membrane. We checked its lack both *in vivo* and in protargol-impregnated specimens (Figs 3, 4, 7, 8, 10 and 11). Thus, the species belongs to the genus

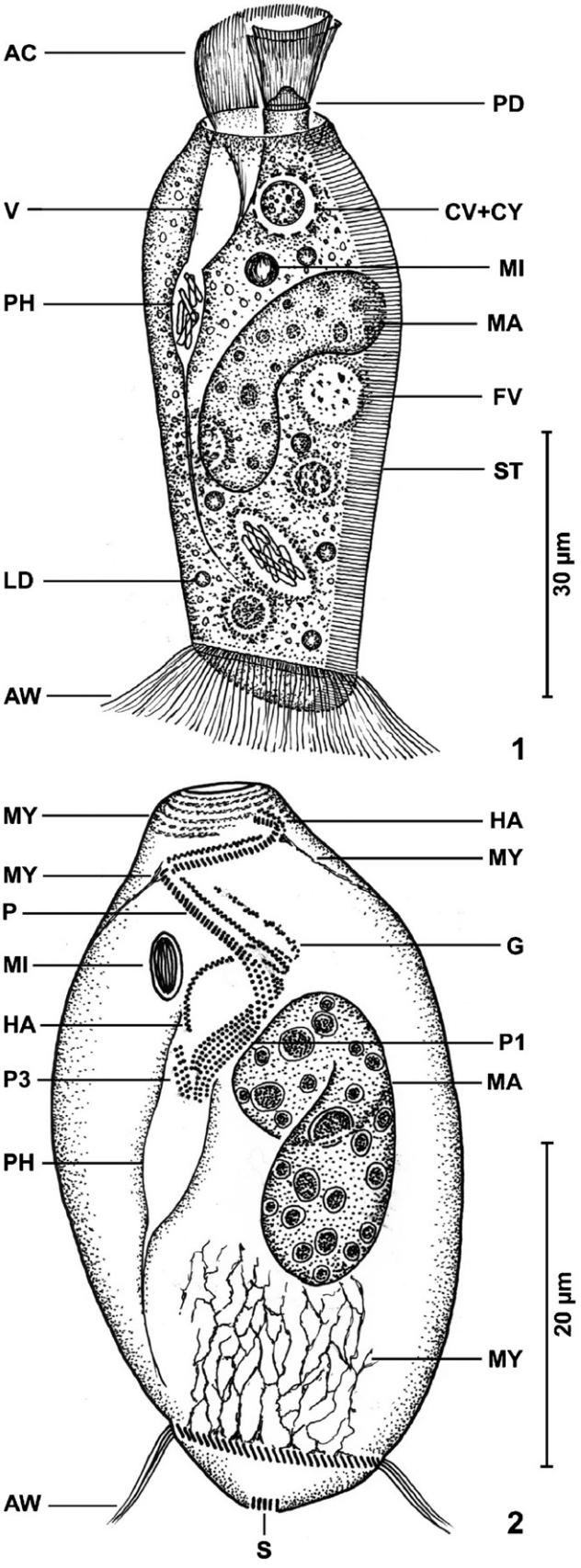


**Figs 1 and 2.** *Telotrochidium matiense* nov. comb. from life (1) and after protargol impregnation (2): (1) General view of a representative specimen. Note that the contractile vacuole and the cytopyge (CV + CY) have almost the same position, the first one lying upon the second one. (2) Ciliary pattern and myoneme system. AC – adoral ciliary spiral, AW – aboral ciliary wreath (trochal band), CV + CY – contractile vacuole and cytopyge, FV – food vacuole, G – germinal (stomatogenic) kinety, HA – haplokinety, LD – lipid droplet, MA – macronucleus, MI – micronucleus, MY – myonemes, P – polykinety, PD – peristomial disk, PH – pharynx, P1, 3 – peniculi, S – scopula, ST – cortical striae corresponding to silverlines, V – vestibulum.

*Telotrochidium*, as defined by Foissner (1975). Accordingly, Figs 4 and 5 in Martín-Cereceda et al. (1999) do not show an epistomial membrane, but part of the oral ciliary spiral, whose cilia are about 10 μm long *in vivo*, that is, they appear rather long when compared with the small body size (Figs 3 and 4).

The second misinterpretation concerns the ventral location of the contractile vacuole (Martín-Cereceda et al. 1999). Indeed, the contractile vacuole is difficult to locate in this species due to the small oral opening, the minute peristomial disc, and the incessant movement of the specimens. Careful observations, micrographs (Figs 3 and 7), and plasticine models suggest that it is located on the dorsal or dorso-lateral wall of the vestibulum and very near to the cytopyge (Figs 4, 8 and 10), which was not observed by Martín-Cereceda et al. (1999).

Further, we checked the appearance of the aboral ciliary wreath in dry silver nitrate-impregnated specimens. It is very similar to that of other *Telotrochidium* species investigated with the same method, that is, there is a row of tightly spaced pellicular pores anterior to and another row posterior to the oblique kineties composing the trochal band (Foissner 1975, 1976, 1978).

The observations on the ciliary pattern match the original description (Figs 2 and 11–13). However, the oral apparatus was slightly to distinctly malformed in about one-third of the specimens, possibly due to the long cultivation of the strain (~10 years). Thus, only cells with clearly visible oral apparatus (Figs 2, 12 and 13) were selected for the following analysis, which was stimulated by the reviewers: of 100 specimens analyzed, 69 had peniculus 3 composed of three basal body rows (Figs 2, 12 and 13); 24 of two rows (Fig. 13; inset); one of five rows; and in six cells peniculus 3 was totally lacking. Further, details of peniculus 3 were also highly variable: the individual ciliary rows may be composed of 3–10 basal bodies; the rows may be of similar (Fig. 12) or of different (Figs 2 and 13) length; and the basal bodies may be highly ordered or rather disordered. As concerns length, peniculus 3 is shorter than peniculus 1 by 1–3 μm, usually 2 μm, posteriorly (proximally). Obviously, peniculus 3 is more variable than widely assumed. Further studies on other populations and species are needed to clarify whether our results are caused by culture effects or fall into the natural range of variability.

The myoneme system is comparatively weakly developed, and thus the specimens do not become globular but ellipsoidal when fully contracted. The myonemes are extraordinary in that they are very fine and form a narrowly meshed reticulum not described in any other peritrich (Fig. 9).

Other minor details (e.g., the location of the trochal ciliary wreath very near to the body end) were also included in the new drawings of the species (Figs 1 and 2). As concerns body shape, it changes from that shown in Figs 1 and 3 to that shown in Martín-Cereceda et al. (1999) when oxygen is depleting.

## Light microscopy of conjugation process

### Preconjugation

Preconjugation division of vegetative cells produces two different sexual morphs: macroconjugants and microconjugants. Macroconjugants are similar to vegetative cells (length: 45–72 μm), whilst microconjugants are much smaller (10–20 μm) and show a typical jerky movement. Microconjugants have a conspicuous trochal band when compared to their small size (Fig. 14). They are able to divide further before initiating conjugation (Fig. 15). In spite of the presence of a vestibulum, they are non-feeding because the peristome is always contracted. The vestibular infraciliature is slightly reduced (Fig. 14) compared to those of the macroconjugant and vegetative cells (Fig. 11).

### Contact

Typically, microconjugants make several attempts to fix onto macroconjugants, bouncing on and off very quickly until they establish contact with their aboral pole (Fig. 16). The union can take place in different areas of the macroconjugant cell surface, generally in the lateral area but never at the aboral pole, i.e., never posterior to the trochal band.

### Microconjugant penetration

The microconjugant penetrates its conjugant mate gradually until it becomes completely enclosed (Figs 17 and 18). This process lasts approximately 30–45 min. By the time of penetration, a mitotic division (preliminary division) occurs in the microconjugant micronucleus, while the macroconjugant micronucleus remains undivided (Fig. 19). At this stage the macronuclei of both conjugants are unaltered, and the cortex of the microconjugant is clearly visible. Occasionally, more than one microconjugant tries to penetrate a macroconjugant (Fig. 19), but these attempts cease once micronucleus pregamic division takes place in the microconjugant that is already inside.

### Pregamic divisions

The micronuclei undergo two meiotic (pregamic) divisions, which are synchronised for both conjugants (Figs 20 and 21). Usually, each micronucleus performs two pregamic divisions, producing four haploid nuclei in the macroconjugant and eight haploid nuclei in the microconjugant (Fig. 22). However, we have also observed that the second pregamic division may occur in only two of the four nuclei of the microconjugant,

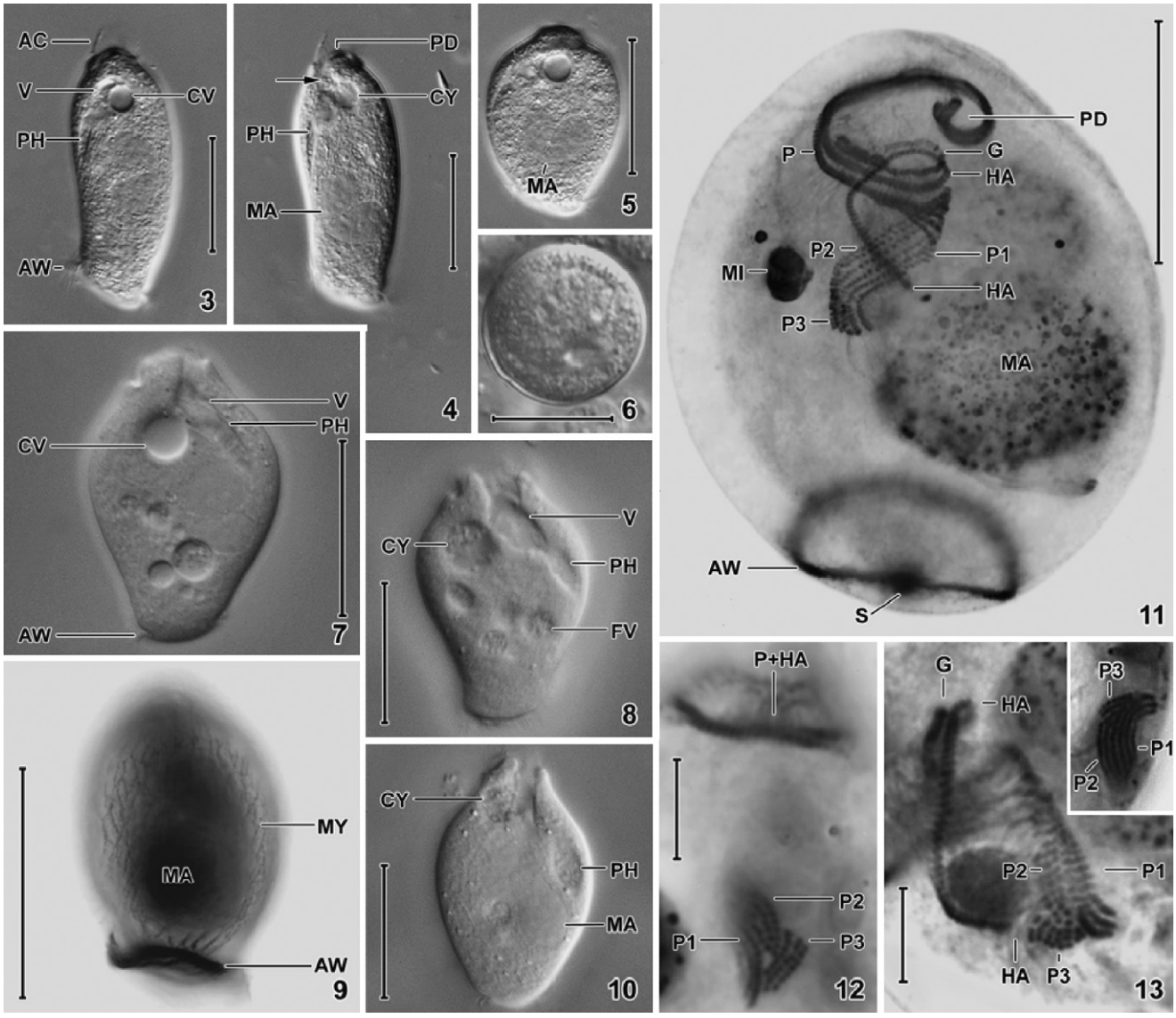


**Figs 3–13.** *Telotrochidium matiense* from life (3–8, 10) and after protargol impregnation (9, 11–13): (3,4) Left side views of a freely motile, cylindrical specimen, showing the contractile vacuole (CV) and the cytopyge (CY) one upon the other on the dorsal wall of the vestibulum, as recognizable by the ventrally located pharynx (PH). Arrow in Fig. 4 marks a fecal mass just leaving the cytopyge. (5) Contracted specimens are not globular, likely due to the weakly developed myoneme system (cf. Figs 2 and 9). (6) Resting cysts are globular and have a thin, smooth wall. (7, 8) Amphoriform, sitting specimen showing the contractile vacuole and the cytopyge on the dorsal wall of the vestibulum (cf. Figs 3 and 4). (9) Surface view showing the fine, reticulate myoneme system. (10) An ellipsoidal specimen just extruding indigestible material via the cytopyge. (11) A heavily squashed specimen showing the oral and somatic ciliary pattern. (12, 13) Proximal end and proximal half of the adoral ciliary spiral, showing that peniculus 2 ends subterminally between peniculi 1 and 3, each composed of three kineties. The inset in Fig. 13 shows a specimen with peniculus 3 composed of only two rows of basal bodies. AC – adoral ciliary spiral, AW – aboral ciliary wreath (trochal band), CV – contractile vacuole, CY – cytopyge, FV – food vacuole, G – germinal (stomatogenic) kinety, HA – haplokinety, MA – macronucleus, MI – micronucleus, MY – myonemes, P – polykinety, PD – peristomial disk, PH – pharynx, P1, 2, 3 – peniculi, S – scopula, V – vestibulum. Scale bars 5 μm (12, 13), 20 μm (6), and 30 μm (3–5, 7–11).

and in only one of the two nuclei of the macroconjugant, thus forming six haploid nuclei in total. Macronuclei start to degenerate after the first pregamic division, and appear intermingled when the second pregamic division has occurred (Fig. 22). The microconjugant cortex disappears and cytoplasmic continuity is established between the conjugants during the second pregamic division. All haploid nuclei except one for each conjugant degenerate eventually. The two conserved haploid nuclei (pronuclei) are easy to recognize because

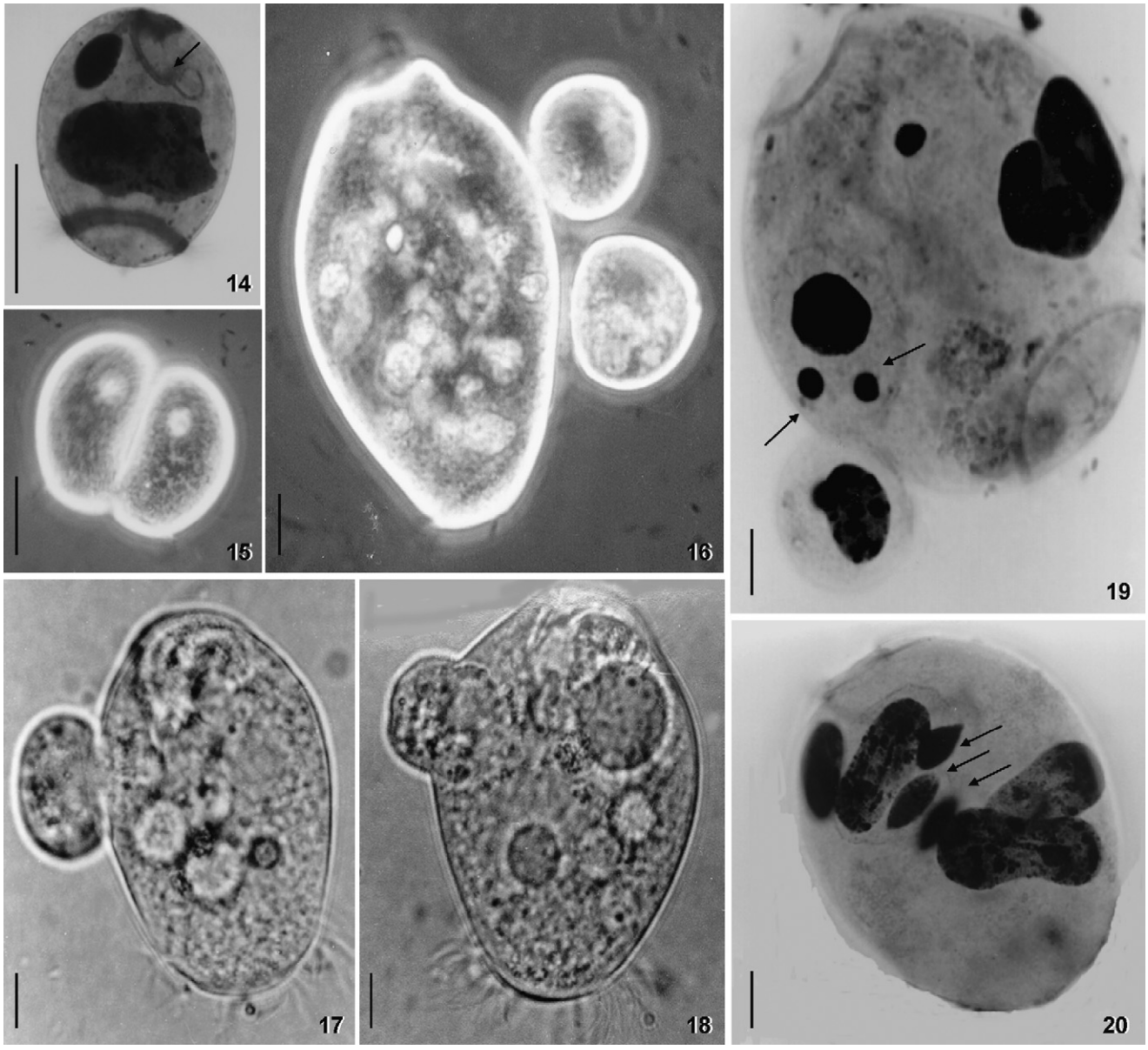


**Figs 14–20.** Initial stages in the conjugation of *Telotrochidium matiense*, *in vivo* (15–18) and after silver carbonate impregnation (14, 19, 20). (14) General view of a microconjugant. Arrow marks oral infraciliature. (15) Microconjugants in amitotic division. (16) Two microconjugants attaching laterally to the macroconjugant. (17, 18) Penetration of the microconjugant into the macroconjugant. (19) First mitotic (preliminary) division of the microconjugant micronucleus (arrows). (20) First pregamic division of micronuclei of both macro- and microconjugant. Arrows mark early dividing nuclei. Bars represent 10 μm.

they are lightly impregnated compared with the rest of haploid nuclei (marked by asterisks in Fig. 22).

### Synkaryon formation

Fusion of the two pronuclei produces the synkaryon (zygote nucleus), which initially appears frayed (Fig. 23), and later assumes a more compact appearance (Fig. 24). The synkaryon is found in either the aboral or the oral area of postconjugant cells. Macronuclear degeneration continues, and numerous globular fragments are produced during synkaryon maturation (Fig. 24).

### Postzygotic divisions

The synkaryon undergoes two postzygotic divisions producing four diploid nuclei (Figs 25 and 26). Occasionally, a third division may occur in postconjugant cells.

### Segregation divisions

One of the diploid nuclei produced during the synkaryon divisions condenses, giving rise to the micronucleus, while the others become macronuclear anlagen. The micronucleus is strongly impregnated, while the macronuclear anlagen stain weakly (Figs 27 and 28).

We have observed the formation of three anlagen, which agrees with the occurrence of two postzygotic divisions. The three anlagen segregated to daughter cells by successive binary (regulation) divisions produce cells with a micronucleus, and each with one (Fig. 29) or two macronuclear anlagen.

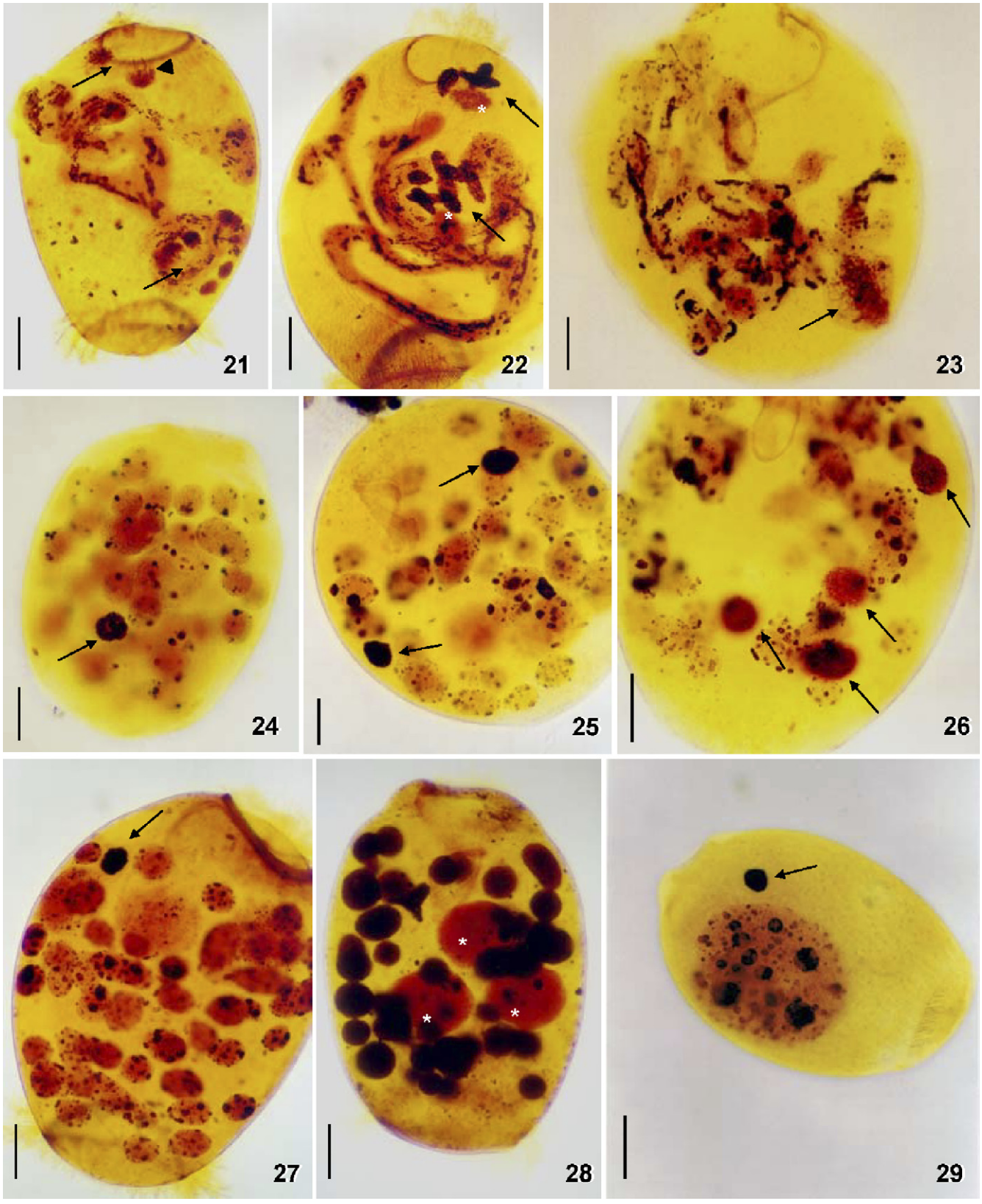

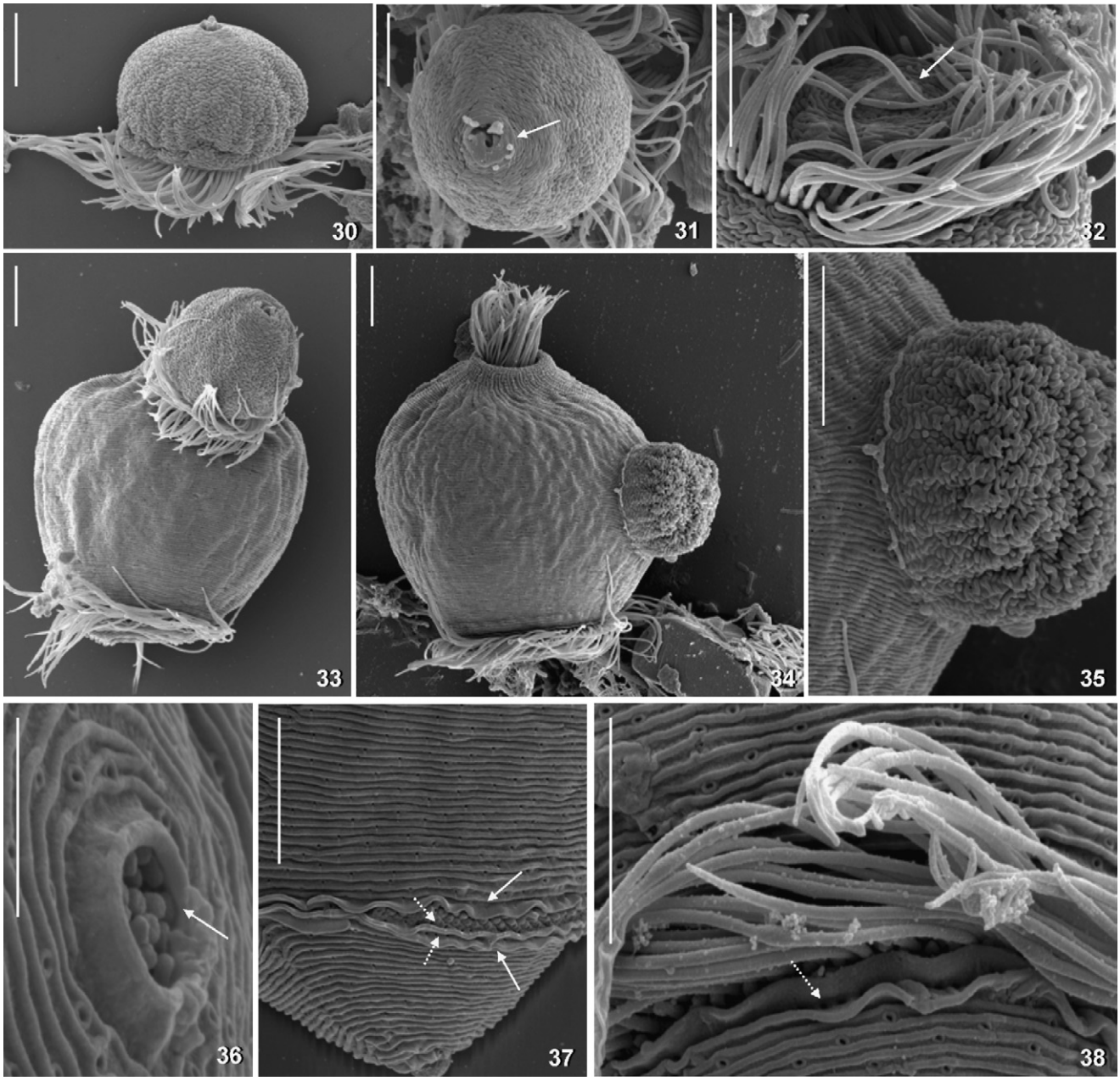


**Figs 30–38.** Scanning electron micrographs of *Telotrochidium matiense*. (30) Microconjugant. Note the conspicuous trochal cilia. (31) Apical view of a microconjugant showing the contracted peristome (arrow). (32) Aboral view of a microconjugant showing the inconspicuous scopula (arrow). (33) Initial stage of conjugation process. Note that the microconjugant attaches laterally to the macroconjugant and that both still have the aboral ciliary wreath. (34, 35) Late stage of conjugation. The microconjugant lost the trochal cilia and penetrates into the macroconjugant. (36) Scopula (arrow) of a macroconjugant. (37, 38) Vegetative cells of *T. matiense* showing the trochal band area. Note the three pellicular folds limiting the trochal band (arrows), and the aboral rows of pores (dotted arrows). Bars represent 10 μm in Figs 30–35 and 5 μm in Figs 36–38.

**Figs 21–29.** Late stages in the conjugation of *Telotrochidium matiense* after silver carbonate impregnation. See text for detailed explanation. (21) Final step in the first pregamic division of micronuclei of both macro- and microconjugant. Arrows mark divided nuclei. Arrowhead indicates nuclei in anaphase. (22) Second pregamic division. Arrows mark nuclei and asterisks denote the two pronuclei. (23, 24) Synkaryon formation. Arrows mark the synkaryon. (25, 26) Postzygotic divisions. Arrows mark the diploid nuclei. (27, 28) Postconjugant cells showing the micronucleus (arrow in Fig. 27) and three macronucleus anlagen (asterisks in Fig. 28). Numerous degeneration fragments of the old macronuclei are still visible at this stage (dark globules in Fig. 28). (29) Segregation division. Daughter cell with a micronucleus (arrow) and one macronucleus anlagen. Bars represent 10 μm.

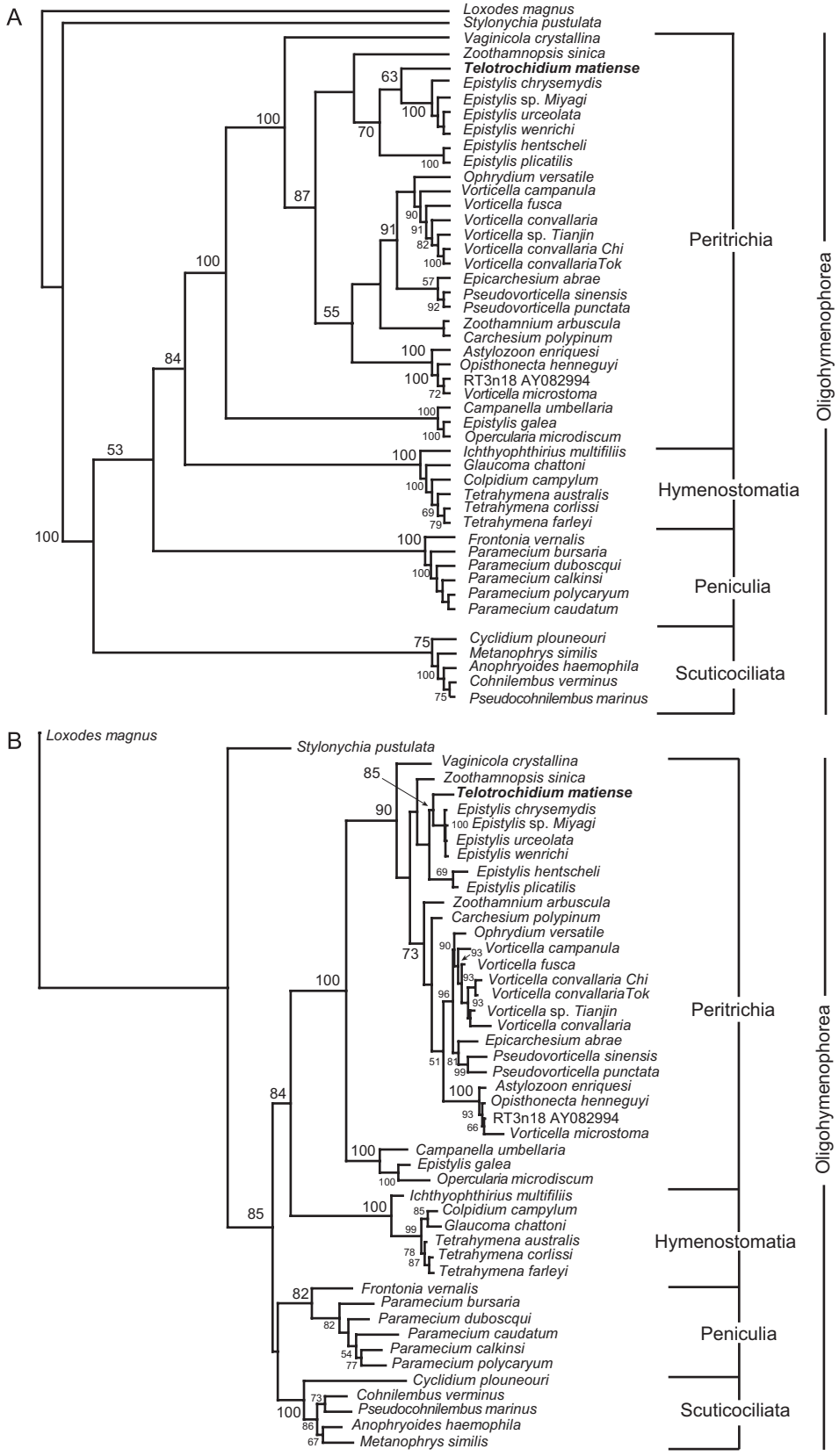


**Fig. 39.** Phylogenetic trees of ciliates inferred from the small subunit ribosomal RNA gene (SSU rDNA) sequences. Species in bold denote the newly sequenced *T. matiense*. (A) 50% majority rule consensus tree obtained via maximum parsimony. Numbers at nodes represent bootstrap values. (B) Maximum likelihood tree. Numbers at nodes represent bootstrap values. Bootstrap values less than 50% are not shown.

### Scanning electron microscopy (SEM) of conjugating and vegetative cells

SEM shows that microconjugants have a trochal band with ordinary cilia, about 15 μm long cilia; a permanently contracted peristome; cortical grooves perforated by pores; and a scopula (Figs 30–32). In spite of the presence of a vestibulum, peristomial cilia are absent (Figs 14, 30 and 31). When conjugation commences, the trochal cilia do not disappear in either of the conjugants (Fig. 33), in contrast to other peritrichs (Clamp and Coats 2000). When conjugation reaches a more advanced stage, the microconjugant trochal cilia are lost (Figs 34 and 35), facilitating the union to macroconjugants (Fig. 35). Macroconjugant trochal cilia persist throughout the conjugation process (Figs 33 and 34). The microconjugant cortex appears to be shrunken, compared to macroconjugants and vegetative cells, mainly when penetrating into the macroconjugant (Fig. 35). This is due to the considerable cellular changes that the microconjugant has to undergo in order to penetrate the macroconjugant, such as breakdown of cellular structures and size reduction. The ciliature and the short bristles of the scopula are clearly visible throughout the entire conjugation process in macroconjugants (Fig. 36), while reduced to minute structures in microconjugants (Fig. 32).

SEM also reveals further ultrastructural features not mentioned by Martín-Cereceda et al. (1999). Pellicular pores visible over the entire cell surface (Figs 35 and 37) correspond to the argyrophilic dots in the pellicle reported by Martín-Cereceda et al. (1999). One oral cortical fold and two aboral cortical folds enclose the trochal band (Figs 37 and 38). Two rows of pellicular pores are visible in the SEM, one above the aboral cortical folds and a second one between the aboral cortical folds (Figs 37 and 38), which confirms the transmission electron microscope observations of Martín-Cereceda et al. (1999).

### SSU rDNA sequence and phylogenetic analyses

The sequence of the SSU rDNA gene (1730 bp) of *T. matiense* was deposited under accession number AY611065 as *O. matiensis* in GenBank on 28/4/2004. MP and ML produce similar tree topologies (Fig. 39) when *Loxodes magnus* (Karyorelictea) and *Stylonychia pustulata* (Spirotrichea) are chosen as outgroups to test the phylogenetic relationships within the class Oligohymenophorea. Our results confirm the monophyly of the Oligohymenophorea (100% MP and 85% ML bootstrap support). Four distinct clades corresponding to the four subclasses of Oligohymenophorea are obtained. Peritrichs and hymenostomes form a well-supported group (84% MP, 84% ML). Support for the monophyly of the subclasses is as follows: Scuticociliatia (75% MP, 100% ML), Peniculia (100% MP, 82% ML), Hymenostomatia (100% MP and 100% ML), and Peritrichia (100% MP, 100% ML).

In both analyses the subclass Peritricha shows rather similar phylogenetic relationships. *Campanella umbellaria*, *Epistylis galea*, and *Opercularia microdiscum* form a monophyletic group (100% MP, 100% ML) sister to all other Peritrichia. *Vaginicola crystallina* is sister to a large clade (87% MP, <50% ML) including the rest of the Peritrichia. Within this clade, we recover three major groups: one encompasses all *Epistylis* species (except *E. galea*) together with *T. matiense* and *Zoothamnopsis sinica*; within this group, *T. matiense* forms a clade with four species of *Epistylis* (*E. chrysemydis*, *E.* sp. Miyagi, *E. urceolata*, and *E. wenrichi*; 63% MP, 85% ML); the second group contains all species of *Vorticella* (except *V. microstoma*), *Ophrydium*, *Epicarchesium*, and *Pseudovorticella* (91% MP, 96% ML); and the third group includes *Astylozoon enriquesi*, *O. henneguyi*, RT3N18, and *Vorticella microstoma* (100% MP, 100% ML). The position of *Zoothamnium arbuscula* and *Carchesium polypinum* varies between trees and is never supported by more than 50% bootstrap.

## Discussion

### Emended diagnosis and comparison of *Telotrochidium matiense* with related species

Foissner (1975) revised the free-swimming sessilids and recognized two genera in the family Opisthonectidae Foissner 1975: *Opisthonecta* (with epistomial membrane and a row of narrowly spaced pellicular pores along the aboral side of the trochal band) and *Telotrochidium* (without epistomial membrane and a row of narrowly spaced pellicular pores along the oral as well as aboral side of the trochal band). Our population matches the diagnosis of *Telotrochidium* (Figs 1–13): the specimens lack an epistomial membrane (see Result section for an explanation of the epistomial membrane described by Martín-Cereceda et al. 1999) and possess two rows of argyrophilic pores, one each above and below the trochal band, as revealed using dry silver nitrate impregnation (Martín-Cereceda et al. 1999). Thus, we transfer *O. matiensis* Martín-Cereceda, Serrano and Guinea, 1999 to the genus *Telotrochidium*: *T. matiense* (Martín-Cereceda et al. 1999) nov. comb., and provide the following emended diagnosis: *in vivo* about 60 × 30 μm; cylindroid to amphoriform, ventral side slightly shorter than dorsal. Macronucleus in midbody, about as long as body width, ends usually slightly inflated. Contractile vacuole and cytopyge on dorsal wall of vestibulum. On average, 129 silverlines from

anterior end of cell to aboral ciliary wreath and 18 silverlines from aboral ciliary wreath to scopula. Oral apparatus opercullariform, i.e., with minute oral disc; peniculus 2 shortened proximally, peniculus 3 composed of three ciliary rows.

Three valid *Telotrochidium* species have been described: *Telotrochidium johanninae* Fauré-Frémiet 1950 (type of genus by subsequent designation; Foissner 1975); *Telotrochidium elongatum* Foissner 1975; and *Telotrochidium cylindricum* Foissner 1978. *T. matiense* is most similar to *T. johanninae*, that is, both have similar size, body shape and macronucleus, as well as an almost identical number of silverlines (for an overview, see Martín-Cereceda et al. 1999). However, they differ in an important feature, viz., in the location of the contractile vacuole which was not established in the original description (Fauré-Frémiet 1950): ventral in *T. johanninae* (Foissner 1976), dorsal in *T. matiense* (Figs 1, 3 and 7). Note that Foissner (1978) stated that the contractile vacuole and the cytopyge of *T. johanninae* are likely to be on the dorsal vestibular wall. However, this paper was written long before, but published later than Foissner (1976), who rediscovered and studied *T. johanninae,* finding the contractile vacuole indeed on the ventral wall of the vestibulum. *T. elongatum* is larger (80–145 μm) than *T. matiense* (45–80 μm), but has much fewer silverlines ($\times 95$ vs. 147) and has both the contractile vacuole and the cytopyge on the ventral wall of the vestibulum (vs. dorsal). *T. cylindricum* is also distinctly larger (130–170 μm) than *T. matiense* (45–80 μm); it has a long, rod-shaped macronucleus along the main body axis (vs. short and in mid-body); and possesses a comparatively large (vs. small) peristomial disc. Further, peniculus 2 is not shortened proximally (Berger et al. 1984).

## Conjugation

*T. matiense* offers an example of total conjugation (heteromorphic monozygotic conjugation), which is widespread among peritrichs. In *T. matiense*, the details of the conjugation process show some variations from those established in other peritrichs (Dass 1953, 1954a, b; Finley 1943; Rosenberg 1940; Sola et al. 1989). In stalked peritrichs (*Carchesium*, *Epistylis*, *Zoothamnium* and *Vorticella*), penetration of the microconjugant occurs through the aboral pole, i.e., close to the peduncle of the macroconjugant, and only the cytoplasm penetrates into the partner. By contrast, in *T. matiense* the microconjugant never attempts to fix to or to penetrate the macroconjugant posterior to the trochal band; moreover, the entire microconjugant penetrates the macroconjugant (Figs 16–19, 33 and 34). In free-swimming sessilids, the only other species studied in detail is *O. henneguyi* (Rosenberg 1940; Sola et al. 1989), in which the microconjugant also penetrates entirely into the macroconjugant mate, but the point of entry is at the aboral tip (scopula), i.e., at the insertion point of the stalk in attached peritrichs.

The transfer of *O. matiensis* to the genus *Telotrochidium* is supported not only by the lack of an epistomial membrane (diagnostic character of *Opisthonecta*), but also by the mode of conjugation and by its SSU rDNA (see below). Foissner (1976, 1978) reported that *O. minima* penetrates the aboral pole, as does *O. henneguyi*, while the microconjugant penetrates laterally in *T. cylindricum*, *T. johanninae* and *T. matiense* (Figs 16–19, 33 and 34). This is further supported by the fact that in *Epistylis alpestris*, the microconjugant has the same insertion point to the macroconjugant as the *Telotrochidium* species mentioned above (Foissner 1978). Thus, Foissner (1978) suggested that differences in the conjugation process may provide important clues towards understanding phylogenetic relationships within the Opisthonectidae and between stalked Peritrichia and Opisthonectidae. Unfortunately, no information on sexual reproduction is available for *Epistylis* species clustering with *T. matiense* in our phylogenetic trees.

Regarding the number of micronuclear pregamic divisions, *T. matiense* is as *O. henneguyi* since two divisions take place, often in all the haploid nuclei, as observed by Rosenberg (1940) in *O. henneguyi*. Like Sola et al. (1989) and Rosenberg (1940), we observed that, at times, the second pregamic division could take place in only one macroconjugant nucleus and two microconjugant nuclei, thus producing six instead of eight haploid nuclei.

The conjugation of peritrichs differs from that of most other Oligohymenophorea, as there is not reciprocal fertilization with separation of two postconjugants. Moreover, the sexual dimorphism, in which the macronucleus and the cytoplasm are divided unequally between the two daughter cells (Dass 1953, 1954a, b; Finley 1943; Ng 1990), is unique to peritrichs. Another special feature of the peritrichs is that preconjugation mitosis of the microconjugant occurs prior to meiosis, although this has been observed also in some hypotrichs (*Euplotes*, *Pseudourostyla*) where it has been related to overlapping asexual and sexual cycles (Ng 1990).

## Phylogenetic analyses

Greenwood et al. (1991) obtained with *O. henneguyi* the first SSU rDNA sequence for peritrichs, which supported the distinctiveness of peritrichs from other ciliates. Miao et al. (2001) sequenced the SSU rDNA of several other peritrichs and found that these were grouped in two clades: a clade with *O. henneguyi* and *Vorticella* species, which was the sister taxon of a second clade made of *Epistylis* species. Moreover, *Vorticella*

*convallaria* grouped closer to *O. henneguyi* than to any other *Vorticella* species. Itabashi et al. (2002) added a third clade to the phylogenetic tree of peritrichs, composed of only *C. polypinum*, set apart from the rest of peritrichs. *V. microstoma* grouped with *O. henneguyi* as we have also observed, and not with *V. convallaria*. Those authors shed doubt on the monophyly of the genus *Vorticella* and concluded that more molecular information is necessary to clarify the relationships between *Vorticella* species and *O. henneguyi*. Miao et al. (2004) confirmed that *O. henneguyi* and *V. microstoma* grouped together, and also highlighted a strong association of *Opisthonecta* with *Astylozoon*, as we also have found. Those authors suggested that *O. henneguyi* is not the ancestor of the stalked peritrichs, because *Astylozoon* has rigid aboral bristles which are considered to be evolutionary relicts of a stalk.

To date, all molecular phylogenetic information for the family Opisthonectidae, established by Foissner (1975), is based on only one *Opisthonecta* species, i.e., *O. henneguyi*. The present study was conceived to contribute to understanding the phylogenetic relationships within the family Opisthonectidae and extensively within the subclass Peritrichia, by improving the phylogenetic tree with a new SSU rDNA sequence for the family (Fig. 39). Our results show that the two genera of the family Opisthonectidae are only distantly related to each other, i.e., *T. matiense* is most closely related to species of *Epistylis*, while *O. henneguyi* is closely related to *A. enriquesi*, *V. microstoma*, and clone RT3n18, an unidentified eukaryote from an extreme (acidic) environment (Amaral-Zettler et al. 2002). This shows that *Telotrochidium* and *Opisthonecta* are derived from different lineages of stalked peritrichs: *Opisthonecta* could have evolved from peritrichs with a contractile stalk (vorticellids), and *Telotrochidium* from peritrichs with a non-contractile stalk (epistyliids or operculariids).

In the most recent peritrich phylogenetic trees, species traditionally placed within the same family, and even within the same genus, do not always cluster together, suggesting that the generic and intrageneric phylogeny needs to be reinterpreted. Miao et al. (2001) and Itabashi et al. (2002) showed that the species of *Vorticella* did not all group together, and Miao et al. (2004) found that *E. galea* diverged from the *Epistylis* clade and closely grouped with *O. microdiscum* and *C. umbellaria*, as we have also observed (Fig. 39). Recently, Clamp and Williams (2006) have shown that *Zoothamnium* is a highly diverse genus with species grouping in four different phylogenetic clades.

Considering these problems, classification changes should be based on more detailed data, especially also on other genes, although it is obvious that *Opisthonecta* and *Telotrochidium* belong to different lineages. Further, are the various *Opisthonecta* and *Telotrochidium* species monophyletic? Is *T. matiense* more closely related to the epistyliids, as indicated by the molecular data; or to the opercullariids, as indicated by the minute peristomial disc and the weakly developed myonemes? These and other questions highlight the complexity of peritrich systematics and the need for exhaustive morphological and molecular investigations on these ciliates.

## Acknowledgments

Financial support by a Marie Curie Fellowship of the European Community (Contract HPMF-CT-2002-01861 to M.M.-C.) and by the Austrian Science Foundation (W.F.) is greatly acknowledged. This study is dedicated to baby daughter Penélope.

Addendum: During the proof stage of our manuscript, Williams and Clamp (Journal of Eukaryotic Microbiology 54(3): 317-323, 2007) have published a manuscript on the phylogenetic position of *O. matiensis* and *O. minima*. They concurred that *O. matiensis* forms a clade with the species of *Epistylis*.

## References

Amaral-Zettler, L.A., Gomez, F., Zettler, E., Keenan, B.G., Amils, R., Sogin, M.L., 2002. Microbiology: eukaryotic diversity in Spain's River of Fire. Nature 417, 137.

Berger, H., Foissner, W., Adam, H., 1984. Taxonomie, Biometrie und Morphogenese einiger terricoler Ciliaten (Protozoa: Ciliophora). Zool. Jb. Syst. 11, 339–367.

Cavalier-Smith, T., 2004. Only six kingdoms of life. Proc. R. Soc. London, Ser. B 271, 1251–1262.

Cavalier-Smith, T., Chao, E.E.Y.P., 2006. Phylogeny and megasystematics of phagotrophic heterokonts (Kingdom Chromista). J. Mol. Evol. 62, 388–420.

Clamp, J.C., Coats, W., 2000. *Planeticovorticella finleyi* n.g., n.sp. (Peritrichia, Vorticellidae) a planktonic ciliate with a polymorphic life cycle. Invert. Biol. 119, 1–16.

Clamp, J.C., Williams, D., 2006. A molecular phylogenetic investigation of *Zoothamnium* (Ciliophora, Peritrichia, Sessilida). J. Eukaryot. Microbiol. 53, 397–403.

Dass, C.M.S., 1953. Studies on the nuclear apparatus of peritrichous ciliates 1. The nuclear apparatus of *Epistylis articulata*. Proc. Natl. Inst. Sci. India 19, 389–404.

Dass, C.M.S., 1954a. Studies on the nuclear apparatus of peritrichous ciliates 1. The nuclear apparatus of *Epistylis* sp. Proc. Natl. Inst. Sci. India 19, 703–715.

Dass, C.M.S., 1954b. Studies on the nuclear apparatus of peritrichous ciliates 1. The nuclear apparatus of *Carchesium spectabile*. Proc. Natl. Inst. Sci. India 20, 174–186.

Elwood, H.J., Olsen, G.J., Sogin, M.L., 1985. The small-subunit ribosomal RNA gene sequences from the hypotrichous ciliates *Oxytricha nova* and *Stylonychia pustulata*. Mol. Biol. Evol. 2, 399–410.

Embley, T.M., Finlay, B.J., Thomas, R.H., Dyal, P.L., 1992. The use of rRNA sequences and fluorescent probes to investigate the phylogenetic positions of the anaerobic

ciliate *Metopus palaeformis* and its archaeobacterial endosymbiont. J. Gen. Microbiol. 138, 1479–1487.

Embley, T.M., Finlay, B.J., Dyal, P.L., Hirt, R.P., Wilkinson, M., Williams, A.G., 1995. Multiple origins of anaerobic ciliates with hydrogenosomes within the radiation of aerobic ciliates. Proc. R. Soc. London Ser B 262, 87–93.

Fauré-Frémiet, E., 1906. Sur une nouvelle vorticellide, *Opisthonecta henneguyi*. C r. hebd. Séanc. Acad. Sci. Paris 60, 922–923.

Fauré-Frémiet, E., 1950. Une nouvelle vorticellide libre, *Telotrochidium johanninae* n.sp. Bull. Soc. Zool. Fr. 75, 148–150.

Felsenstein, J., 1985. Confidence limits on phylogenies: an approach using the bootstrap. Evolution 39, 783–791.

Fernández-Galiano, D., 1994. The ammoniacal silver carbonate method as a general procedure in the study of protozoa from sewage (and other) waters. Water Res. 28, 495–496.

Finley, H.E., 1943. The conjugation of *Vorticella microstoma*. Trans. Am. Microsc. Soc. 62, 97–121.

Foissner, W., 1975. Opisthonectidae (Ciliata, Peritrichida) nov. fam. und Revision der Genera *Telotrochidium* (Kent) und *Opisthonecta* (Fauré-Frémiet). Protistologica 11, 395–414.

Foissner, W., 1976. Eine Neubeschreibung von *Telotrochidium johanninae* Fauré-Frémiet, 1950 (Ciliata, Opisthonectidae). Protistologica 12, 263–269.

Foissner, W., 1978. *Opisthonecta bivacuolata* nov. spec., *Telotrochidium cylindricum* nov. spec. und *Epistylis alpestris* nov. spec., drei neue peritriche Ciliaten aus dem Hochgebirge. Annln naturh. Mus. Wien 81, 549–565.

Foissner, W., 1991. Basic light and scanning electron microscopic methods for taxonomic studies of ciliated protozoa. Eur. J. Protistol. 27, 313–330.

Fuhrman, J.A., Comeau, D.E., Hagström, Å., Chan, A.H., 1988. Extraction from natural planktonic microorganisms of DNA suitable for molecular biological studies. Appl. Environ. Microbiol. 54, 1426–1429.

Gong, Y.C., Yu, Y.H., Villalobo, E., Zhu, F.-Y., Miao, W., 2006. Reevaluation of the phylogenetic relationship between mobilid and sessilid peritrichs (Ciliophora, Oligohymenophorea) based on small subunit rRNA genes sequences. J. Eukaryot. Microbiol. 53, 397–403.

Greenwood, S.J., Sogin, M.L., Lynn, D.H., 1991. Phylogenetic relationships within the Class Oligohymenophorea, Phylum Ciliophora, inferred from the complete small subunit rRNA gene sequences of *Colpidium campylum, Glaucoma chattoni*, and *Opisthonecta henneguyi*. J. Mol. Evol. 33, 163–174.

Hirt, R.P., Dyal, P.L., Wilkinson, M., Finlay, B.J., Roberts, D.M., Embley, T.M., 1995. Phylogenetic relationships among karyorelictids and heterotrichs inferred from small subunit rRNA sequences: resolution at the base of the ciliate tree. Mol. Phylogenet. Evol. 3, 77–87.

Itabashi, T., Mikami, K., Fang, J., Asai, H., 2002. Phylogenetic relationships between *Vorticella convallaria* and other species inferred from small subunit rRNA gene sequences. Zool. Sci. 19, 931–937.

Kent, W.S., 1880–1882. A Manual of the Infusoria, vols. I–III. David Bogue, London, 913pp.

Lynn, D.H., Gransden, S.G., Wright, A.-D.G., Josephson, G., 2000. Characterization of a new species of the ciliate *Tetrahymena* (Ciliophora: Oligohymenophorea) isolated from the urine of a dog: first report of *Tetrahymena* from a mammal. Acta Protozool. 39, 289–294.

Maddison, D.R., Maddison, W.P., 2000. MacClade: Analysis of Phylogeny and Character Evolution. Vers. 4.0. Sinauer, Sunderland, MA.

Martín-Cereceda, M., Serrano, S., Guinea, A., 1999. Description of *Opisthonecta matiensis* n. sp. (Protozoa, Ciliophora), a new peritrich ciliate from wastewater. J. Eukaryot. Microbiol. 46, 283–289.

Miao, W., Yu, Y.H., Shen, Y.H., 2001. Phylogenetic relationships of the subclass Peritrichia (Oligohymenophorea, Ciliophora) with emphasis on the genus *Epistylis*, inferred from small subunit rRNA gene sequences. J. Eukaryot. Microbiol. 48, 583–587.

Miao, W., Yu, Y.H., Shen, Y.F., Zhang, X.Y., 2002. Phylogenetic relationships among six species of *Epistylis* inferred from 18S-ITS1 sequences. Sci. China Ser. C 45, 280–288.

Miao, W., Feng, W., Yu, Y.H., Zhang, X.Y., Shen, Y.F., 2004. Phylogenetic relationships of the subclass Peritrichia (Oligohymenophorea, Ciliophora) inferred from small subunit rRNA gene sequences. J. Eukaryot. Microbiol. 51, 180–186.

Moon-van der Staay, S.Y., Tzeneva, V.A., van der Staay, G.W.M., de Vos, W.M., Smidt, H., Hackstein, J.H.P., 2006. Eukaryotic diversity in historical soil samples. FEMS Microbiol. Ecol. 57, 420–428.

Ng, S.F., 1990. Developmental heterochrony in ciliated protozoa – overlap of asexual and sexual cycles during conjugation. Biol. Rev. Cambridge Philos. Soc. 65, 19–101.

Page, R.D.M., 1996. TreeView: an application to display phylogenetic trees on personal computers. Comput. Appl. Biosci. 12, 357–358.

Posada, D., Crandall, K.A., 1998. Modeltest: testing the model of DNA substitution. Bioinformatics 14, 817–818.

Ragan, M.A., Cawthorn, R.J., Despres, B., Murphy, C.A., Singh, R.K., Loughlin, M.B., Bayer, R.C., 1996. The lobster parasite *Anophryoides haemophila* (Scuticociliatida: Orchitophryidae): nuclear 18S rDNA sequence, phylogeny and detection using oligonucleotide primers. J. Eukaryot. Microbiol. 43, 341–346.

Rosenberg, L.E., 1940. Conjugation in *Opisthonecta henneguyi*, a free swimming vorticellid. Proc. Am. Philos. Soc. 82, 437–449.

Schlegel, M., 2003. Phylogeny of eukaryotes recovered with molecular data: highlights and pitfalls. Eur. J. Protistol. 39, 113–122.

Shang, H., Song, W., Warren, A., Li, L., Chen, Z., 2006. Phylogenetic positions of two marine ciliates, *Metanophrys similis* and *Pseudocohnilembus hargisi* (Protozoa, Ciliophora, Scuticociliatia), inferred from complete small subunit rRNA gene sequences. Prog. Nat. Sci. 16, 373–378.

Sogin, M.L., Ingold, A., Karlok, M., Nielsen, H., Engberg, J., 1986. Phylogenetic evidence for the acquisition of ribosomal RNA introns subsequent to the divergence of some of the major *Tetrahymena* groups. EMBO J. 5, 3625–3630.

Sola, A., Guinea, A., Fernández-Galiano, D., 1989. Light microscopical study of the conjugation process in *Opistho-*

*necta henneguyi* Fauré-Frémiet (Ciliophora, Peritrichida). Acta Protozool. 28, 239–244.

Strüder-Kypke, M.C., Wright, A.-D.G., Fokin, S.I., Lynn, D.H., 2000. Phylogenetic relationships of the genus *Paramecium* inferred from small subunit rRNA gene sequences. Mol. Phylogen. Evol. 14, 122–130.

Swofford, D.L., 2000. PAUP*. Phylogenetic Analysis Using Parsimony (*and other methods). Vers. 4.0b. Sinauer Associates, Sunderland, MA.

Thompson, J.D., Gibson, T.J., Plewniak, F., Jeanmougin, F., Higgins, D.G., 1997. The CLUSTAL-X windows interface: flexible strategies for multiple sequence alignment aided by quality analysis tools. Nucleic Acids Res. 25, 4876–4882.

Wright, A.-D., Lynn, D.H., 1995. Phylogeny of the fish parasite *Ichthyophthirius* and its relatives *Ophryoglena* and *Tetrahymena* (Ciliophora, Hymenostomatia) inferred from 18S ribosomal RNA sequences. Mol. Biol. Evol. 12, 285–290.

Yang, Z., 1994a. Estimating the pattern of nucleotide substitution. J. Mol. Evol. 39, 105–111.

Yang, Z., 1994b. Maximum likelihood phylogenetic estimation from DNA-sequences with variable rates over sites: appropriate methods. J. Mol. Evol. 39, 306–314.